Annals of Biomedical Engineering, Vol. 44, No. 9, September 2016 (© *2016*) pp. 2805–2816
DOI: 10.1007/s10439-016-1560-3

Development and Validation of a High Anatomical Fidelity FE Model for the Buttock and Thigh of a Seated Individual

RAMI M. A. AL-DIRINI,[1] MATTHEW P. REED,[2] JINGWEN HU,[2] and DOMINIC THEWLIS[3]

[1]School of Computer Science, Engineering and Mathematics, Flinders University, Adelaide, SA 5001, Australia; [2]University of Michigan Transportation Research Institute, University of Michigan, Ann Arbor, MI 48109, USA; and [3]Division of Health Sciences, Sansom Institute for Health Research, University of South Australia, Adelaide, SA 5001, Australia

(*Received 9 June 2015; accepted 1 February 2016; published online 8 February 2016*)

Associate Editor Amit Gefen oversaw the review of this article.

Abstract—Current practices for designing new cushions for seats depend on superficial measurements, such as pressure mapping, which do not provide sufficient information about the condition of sub-dermal tissues. Finite element (FE) modelling offers a unique alternative to integrate assessment of sub-dermal tissue condition into seat/cushion design and development processes. However, the development and validation of such FE models for seated humans requires accurate representation of the anatomy and material properties, which remain challenges that are yet to be addressed. This paper presents the development and validation of a detailed 3D FE model with high anatomical fidelity of the buttock and thigh, for a specific seated subject. The developed model consisted of 28 muscles, the pelvis, sacrum, femur, and one layer of inter-muscular fat, subcutaneous fat and skin. Validation against *in vivo* measurements from MRI data confirmed that the FE model can simulate the deformation of soft tissues under sitting loads with an accuracy of (mean ± SD) 4.7 ± 4.4 mm. Simulation results showed that the maximum strains (compressive, shear and von-Mises) on muscles (41, 110, 79%) were higher than fat tissues (21, 62, 41%). The muscles that experienced the highest mechanical loads were the gluteus maximus, adductor magnus and muscles in the posterior aspect of the thighs (biceps femoris, semitendinosus and semimembranosus muscles). The developed FE model contributes to the progression towards bio-fidelity in modelling the human body in seated postures by providing insight into the distribution of stresses/strains in individual muscles and inter-muscular fat in the buttock and thigh of seated individuals. Industrial applications for the developed FE model include improving the design of office and household furniture, automotive and airplane seats and wheelchairs as well as customisation and assessment of sporting and medical equipment to meet individual requirements.

Keywords—Sub-dermal strains, Soft-tissue deformation, Sitting, MRI, FE simulation.

Address correspondence to Rami M. A. Al-Dirini, School of Computer Science, Engineering and Mathematics, Flinders University, Adelaide, SA 5001, Australia. Electronic mail: rami.aldirini@flinders.edu.au

INTRODUCTION

Technological advancements and changes in work and travel cultures have made sitting the dominant posture for many individuals.[13] This is the case for office workers,[6] drivers[12,31] as well as wheelchair users.[51] Rather paradoxically, this perceived comfortable posture has been shown to be associated with a number of health concerns.[52] While sitting, the weight of the body stresses sub-dermal soft tissues in the buttocks and thighs region, especially under bony prominences.[45] Poor cushion design can elevate these pressures, which compromises the health of the pressured soft tissues leading to discomfort or even injury.[49,58] Therefore, it is important to account for the condition of sub-dermal soft tissues when designing cushions for seats and wheelchairs.[18,34]

Current medical imaging methods may provide some information about the geometry of the different anatomical structures[3,22] and may offer basic information on soft tissue deformation. However, this technology cannot provide detailed information of local stresses and strains, and is difficult to integrate within industrial design processes due to the complex experimental setup and the high costs associated. Computational modelling, especially finite element (FE) modelling, offers an alternative to integrate assessment of sub-dermal tissue condition into seat/cushion design and development processes.[40,43] FE models, with the appropriate level of validation and anatomical detail, can provide information about sub-dermal strains in seated subjects. Such capability can inform the research and development process on how changes in seat design may affect seated individuals, prior to building and testing physical prototypes. However, the development and validation of such FE models requires accurate representation of the anatomy and material properties of the tissues which remain challenges that are yet to be fully addressed.[28]

The anatomical fidelity of FE models used in previous studies varied depending on the detail captured by the model geometry. Many models represent anatomical structures by simplified geometries such as cylinders and spheres, which do not capture the complex geometry of human anatomy.[1,5,7] Recent studies used subject-specific FE models that were developed based on medical images, but with unrealistic constraints such as constraining the deformation of soft tissues to a single plane.[8,22,47] While these assumptions can reduce solution time, their potential to compromise the fidelity of the model's output cannot be overlooked.[46] 3D models of the buttock and thighs have been developed from medical images of subjects in postures other than sitting postures,[9,16,43] however, these fail to accurately describe the orientation of soft tissues in seated individuals.[29] The resolution of previous 3D models is also limited due to the grouping of muscles by compartment[19,27] (or even grouping of fat and muscles together[33,56]), which masks information about the response of individual muscles and enveloping inter-muscular fat to sitting loads. Computational (2D) studies suggest the existence of a relationship between high inter-muscular fat levels and elevated mechanical loads on sub-dermal tissues.[48] These results highlight the need for high fidelity 3D FE models of seated humans that are capable of estimating the sub-dermal strains in individual muscles and inter-muscular fat. Hence, the aim of this study was to develop and validate a 3D FE model for a specific seated subject, with anatomical geometry sufficient to capture the deformation and strains in muscles and inter-muscular fat tissues of the buttock and thigh region. This model will provide insightful information about how the different soft tissues respond to sitting loads, which can aid the design of better seats and supporting surfaces in the future.

MATERIALS AND METHODS

Overview

In this single-subject case study, MRI data of a seated male subject was segmented into individual muscles, inter-muscular and subcutaneous fat, skin, and bones. The segmented MRI data were used to generate a detailed 3D geometry for an FE model of the buttock and thigh. Heuristic optimisation was used to define material model parameter values for muscle and fat components of the model. Boundary and loading conditions were applied to simulate quasi-static sitting loads. The model was used to estimate the deformation and strains in sub-dermal muscle and fat tissues, as well as the pressures at the interface between the subject and the seat. Finally, the model was validated by comparing the FE estimates to physical measurements (from MRI data) of the deformation of the gluteal region soft tissues (Fig. 1).

Geometry Generation

Geometric data describing the anatomy of a seated human buttocks and thighs were extracted from MRI scans of a male subject (Age: 44 years, body mass: 73 kg and stature: 1.71 m). The study protocol was approved by the University of South Australia Human Research Ethics Committee (Protocol Number 0000023194), and the University of Aberdeen, College of Life sciences and Medicine Ethics Review Board. After providing written, informed consent the subject was scanned using a positional MRI scanner (Fonar 0.6 Tesla IndomitableTM) under two loading conditions: weight-bearing and non-weight-bearing conditions. MRI data of the subject's buttock and thighs in the non-weight-bearing condition described the geometry of the subject's buttock and thigh before soft tissues undergo any deformation due to the subject's weight. The weight-bearing MRI scans were used to measure the deformation of the different soft tissue layers. For the weight-bearing condition, the subject was scanned in a recumbent sitting posture. In the non-weight-bearing condition, the subject was asked to adopt the same posture, but on an inclined surface and was supported by a set of cushions to help fixate his posture throughout the scanning. In the non-weight-bearing setup, soft tissues in the buttock and thighs were only under the effect of gravity (details of the experimental setup for the MRI scanning are presented in Al-Dirini *et al.*[3]). Solidworks 2012 (Dassault Systèmes, Vélizy, France) was used to manually segment the MRI scans (resolution: 256×256, pixel spacing (mm): 1.5625×1.5625), in consultation with an experienced radiologist, and generate the subject-specific CAD model. The CAD model (Fig. 2a) had three bony structures (pelvis, sacrum and femur), 28 muscles (Table 1) and one layer consisting of inter-muscular fat, fascia and subcutaneous fat.[2]

FE Model Setup

The generated subject-specific CAD model was imported into ANSYS WorkBench v14.5 (ANSYS, Inc., Canonsburg, PA). It was possible to reduce the model size by assuming symmetry about the mid-sagittal plane passing through the sacrum, so that simulations were only run for the left buttock and thigh. A rectangular flat platform was created underneath the CAD

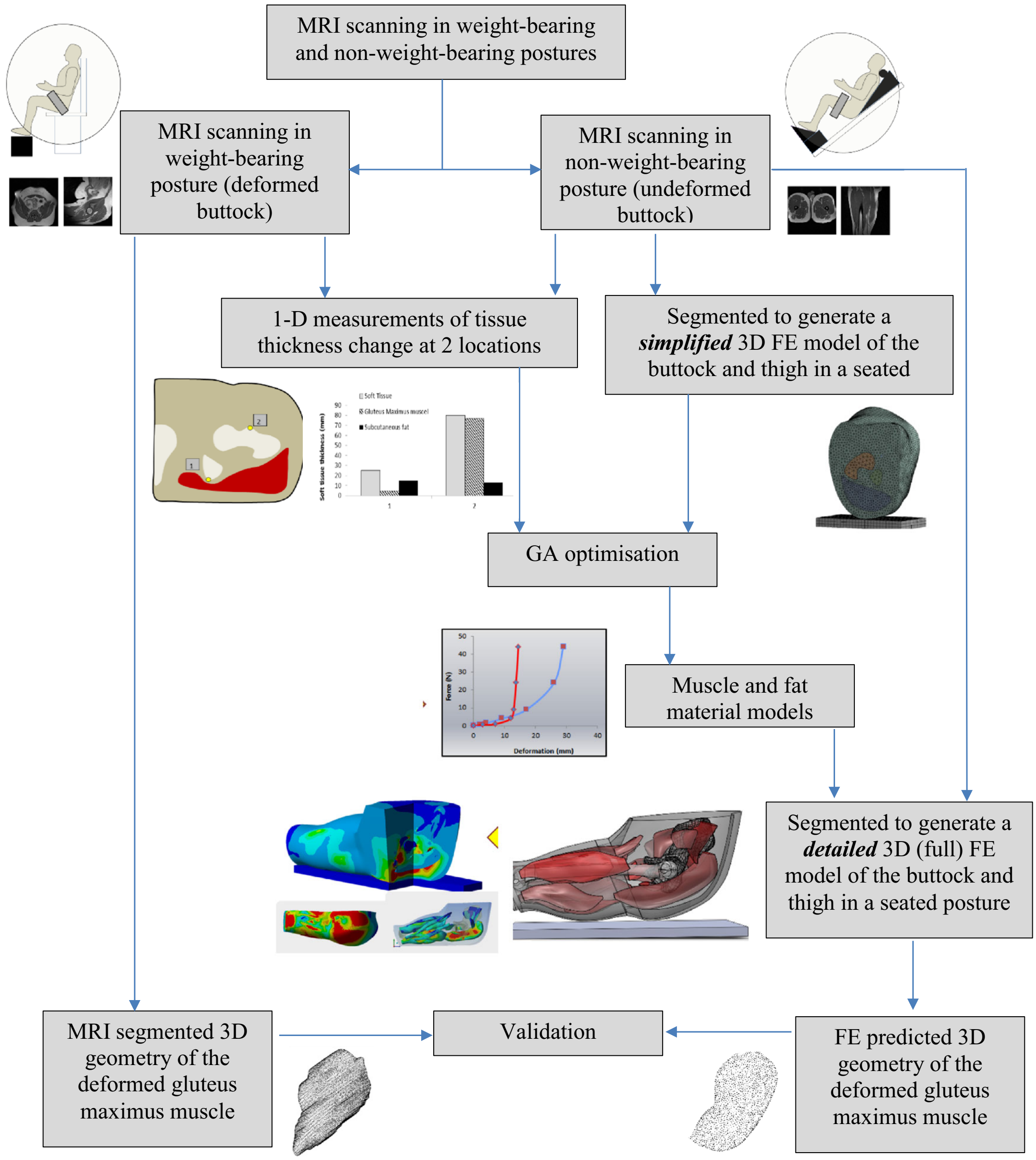

FIGURE 1. Steps for FE model development and validation. (1) MRI scans of undeformed buttock were segmented to generate a detailed 3D FE model. (2) MRI scans of the undeformed buttock were segmented again to generate a simplified FE model. (3) 1-D measurements of tissue thickness changes for the transition from the undeformed (non-weight-bearing) to the deformed (weight-bearing) buttock were taken below the ischial tuberosity and the lesser trochanter in the plane of a single MRI scan. (4) 1-D measurements were used as input for GA optimization to define soft tissue material models. The simplified model is used in GA optimization stage to reduce simulation time. (5) Material models established through the GA optimization were applied to the detailed FE model. (6) MRI scans of the deformed buttock (weight-bearing) were segmented to generate 3D geometry of the deformed gluteus maximus muscle. (7) 3D deformation of the gluteus maximus muscle predicted by the detailed 3D model were compared to those measured from the MRI to validate the detailed model's predictions.

model of the subject's right buttock and thigh representing the seat used in the MRI scanning (Fig. 2). The CAD model (only the left buttock and thigh) and the seat surface were then meshed using ANSYS Mechanical v14.5 (ANSYS, Inc., Canonsburg, PA). The meshed model (Fig. 2) had 255,478 nodes and 1,293,241 tetrahedral elements, with average aspect ratio and skewness of 1.1 and 0.24, respectively. A mesh convergence study was performed to verify the coverage of the model for the adopted mesh density.

Throughout the simulation, isotropic constitutive laws were used to describe the different materials in the

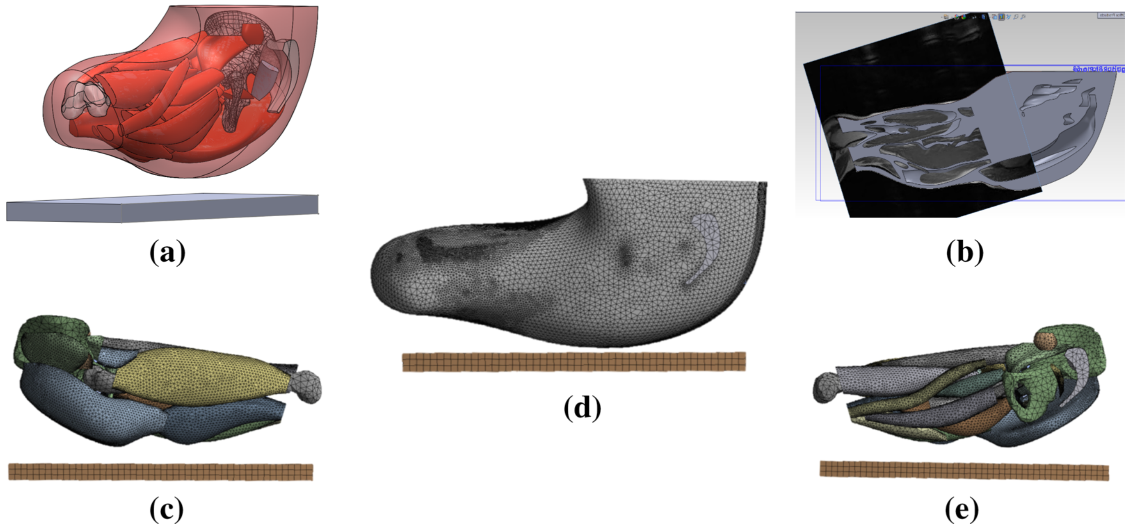

FIGURE 2. Three dimensional CAD model of left buttock and thigh. The model was created from MRI scan segmentation. This included: (1) manual tracing over contours of muscles, fat and bones in transverse MRI scans using Bieser splines in solidworks, (2) creating a lofted geometry that connects the segmentation contours. The path that the loft operation followed was determined from segmentation of sagittal MRI images. The resultant CAD model included detailed geometric representation of each of the buttock and thigh muscles, fat and bones. (a) An isometric view of the 3D subject-specific CAD model. (b) A side view of the 3D subject-specific CAD model overlaid on to the sagittal non-weight-bearing MRI scan of the upper thigh. (c) The right view of the meshed muscles and bones, (d) the left view of the mesh for the fat layer and the sacrum, and (e) the left view of the meshed muscles and bones.

TABLE 1. Summary of muscles modelled in this study.

Gluteus maximus	Tensor of fascia lata	Adductor brevis	Gracilis
Gluteus medius	Biceps femoris	Adductor minus	Iliacus
Gluteus minimus	Rectus femoris	Adductor magnus	Iliopsoas
External oblique	Vastus lateralis	Adductor longus	Sartorius
Internal oblique	Vastus medialis	Obturator externus	Piriformis
Semitendinosus	Vastus intermedialis	Quadratus femoris	Pectineus
Semimembranosus	Gemellus inferior	Obturator internus	Psoas major

model. Bones (ilium, sacrum and femur) were assumed to be rigid, while fat and muscles were modelled using hyper-elastic (first-order Ogden) models with parameter (μ and α) values defined based on genetic algorithm (GA) optimisation (see "Material Model Parameter Optimisation" section for more details). The flat support representing the seat surface was assumed to be rigid. Muscle–bone contacts were defined as frictional contacts with a coefficient of friction (μ_s) of 0.3.[42] A tied/non-slip contact was assigned to all fat–bone[26] and muscle–fat interfaces. Tendons were not independently modelled as the MRI images' resolution and slice interval did not clearly show tendons. The contact between the buttock and the flat support was assumed to be frictional with a coefficient of friction (μ_s) of 0.4.[59] Finally, the seat surface was displaced vertically by 32.3 mm (a distance equal to the maximum total soft tissue thickness change measured from the weight-bearing and none-weight-bearing scans) and gravity was applied throughout the duration of the simulation. ANSYS explicit solver (AUTODYN explicit dynamics module) was used to run the simulations on an Intel Xeon workstation (using 14 processors) with 64 GB RAM. The 95th percentile compressive (3rd principal), maximum shear and von-Mises strains in each of the muscle and fat components of the model were recorded.

Material Model Parameter Optimisation

A linear elastic material model was assigned for the left femur and pelvis.[37] Muscle and subcutaneous fat tissues were modelled as incompressible hyper-elastic materials using first order Ogden models.[35] The general form of the strain energy function for the Ogden model is:

$$W(\lambda_1, \lambda_2, \lambda_3) = \sum_{p=1}^{N} \frac{\mu_p}{\alpha_p}\left(\lambda_1^{\alpha_p} + \lambda_2^{\alpha_p} + \lambda_3^{\alpha_p} - 3\right) + \sum_{p=1}^{N} \frac{1}{d_p}(J-1)^{2p}, \tag{1}$$

where λ_1, λ_2, and λ_3 are the stretch ratios in the principal directions. N is the model order. μ_p, α_p and d_p are the pth shear modulus, exponent and compressibility respectively. J is the determinant of the elastic deformation gradient and can be represented as:

$$J = \lambda_1 \lambda_2 \lambda_3. \tag{2}$$

.

The ground-state shear modulus (μ_0), long-term shear modulus (μ_{inf}) and ground-state bulk modulus (K_0) can be derived using:

$$\mu_0 = \sum_{p=1}^{N} \frac{\mu_p \alpha_p}{2} \tag{3}$$

$$\mu_{\text{inf}} = \sum_{p=1}^{N} \mu_p \tag{4}$$

$$K_0 = \frac{2}{d_1}. \tag{5}$$

Genetic algorithm (GA) optimisation has been used in previous studies to identify model parameter values that best describe the material properties of soft tissues[17] such as the placenta[14] and the liver.[55] In this study, Ogden model parameters for muscle (μ_m and α_m) and subcutaneous fat tissues (μ_f and α_f) were optimised using the adaptive multi-objective optimisation algorithm in ANSYS Workbench's design optimization module (ANSYS, Inc., Canonsburg, PA), which combines GA optimisation with Latin Hypercube sampling.[14] Muscle and fat tissues were modelled as nearly incompressible material, with values of the incompressibility parameters (d_f and d_m) adopted from previous literature.[44] The objective of the optimisation was set to ensure the optimised material models resulted in FE estimates that match MRI measurement of 1-D tissue thickness change for the Gluteus Maximus, intermuscular fat (IMF) and subcutaneous fat[3] below the ischial tuberosity and the lesser trochanter. Thus, the objective for the optimisation was to minimise the following error functions:

$$e_1 = \sqrt{\left(\Delta T_{\text{Muscle\_MRI}_{\text{IT}}}\right)^2 - \left(\Delta T_{\text{Muscle\_FE}_{\text{IT}}}\right)^2} \tag{6}$$

$$e_2 = \sqrt{\left(\Delta T_{\text{Fat\_MRI}_{\text{IT}}}\right)^2 - \left(\Delta T_{\text{Fat\_FE}_{\text{IT}}}\right)^2} \tag{7}$$

$$e_3 = \sqrt{\left(\Delta T_{\text{Muscle\_MRI}_{\text{LT}}}\right)^2 - \left(\Delta T_{\text{Muscle\_FE}_{\text{LT}}}\right)^2} \tag{8}$$

$$e_4 = \sqrt{\left(\Delta T_{\text{Fat\_MRI}_{\text{LT}}}\right)^2 - \left(\Delta T_{\text{Fat\_FE}_{\text{LT}}}\right)^2} \tag{9}$$

$$e_5 = \sqrt{\left(\Delta T_{\text{IMF\_MRI}_{\text{LT}}}\right)^2 - \left(\Delta T_{\text{IMF\_FE}_{\text{LT}}}\right)^2}, \tag{10}$$

where $\Delta T_{\text{Muscle\_MRI}_{\text{IT}}}$, $\Delta T_{\text{Fat\_MRI}_{\text{IT}}}$, $\Delta T_{\text{Muscle\_MRI}_{\text{LT}}}$, $\Delta T_{\text{Fat\_MRI}_{\text{LT}}}$ and $\Delta T_{\text{IMF\_MRI}_{\text{LT}}}$ were the muscle, fat tissue and intermuscular fat 1-D tissue thickness changes below the ischial tuberosity (IT) and the lesser trochanter (LT), respectively, measured from the MRI scans. Similarly, $\Delta T_{\text{Muscle\_FE}_{\text{IT}}}$, $\Delta T_{\text{Fat\_FE}_{\text{IT}}}$, $\Delta T_{\text{Muscle\_FE}_{\text{LT}}}$, $\Delta T_{\text{Fat\_FE}_{\text{LT}}}$ and $\Delta T_{\text{IMF\_FE}_{\text{LT}}}$ were the muscle, fat tissue and intermuscular fat 1-D tissue thickness changes below the ischial tuberosity (IT) and the lesser trochanter (LT), respectively, measured from the FE simulations.

The maximum allowable number of generations was set to 200, with each generation consisting of 50 samples.[14] The initial search space for the Latin Hypercube sampling was defined based on maximum and minimum values for each parameter, which were derived from previous literature[11,20,21,23–25,28]. GA optimisation ceased once all objectives were achieved.[54]

To reduce the size of the model for the optimisation algorithm to converge in a reasonable time, MRI data for each subject were re-segmented into only four anatomical structures (the pelvis, femur, sacrum, GM muscle and fat tissues) to generate a less detailed 3D representation of the buttock (Fig. 3). The 3D geometry with less detail was further reduced to include only tissues surrounding the ischial tuberosity and the lesser trochanter. This was done by creating cut planes to define the part of the 3D geometry to be used for the material optimisation (Fig. 3c). All geometries that were not between the two cut planes were removed. The simplified 3D geometry (Fig. 3c) was meshed using ANSYS workbench v14.5 (ANSYS, Inc., Canonsburg, PA) to generate a pure tetrahedral mesh with the same mesh density of the detailed 3D model.

To simulate the deformation of the buttock's soft tissues, the rectangular block was displaced in the positive y-direction (anterior direction) to deform the buttock model by 32.3 mm, which is equivalent to the total soft tissue deformation measured from the MRI scans. A fixed boundary condition was applied to the bones (Fig. 3c). The simulation ceased when the rigid block was displacement by a total of 32.3 mm.

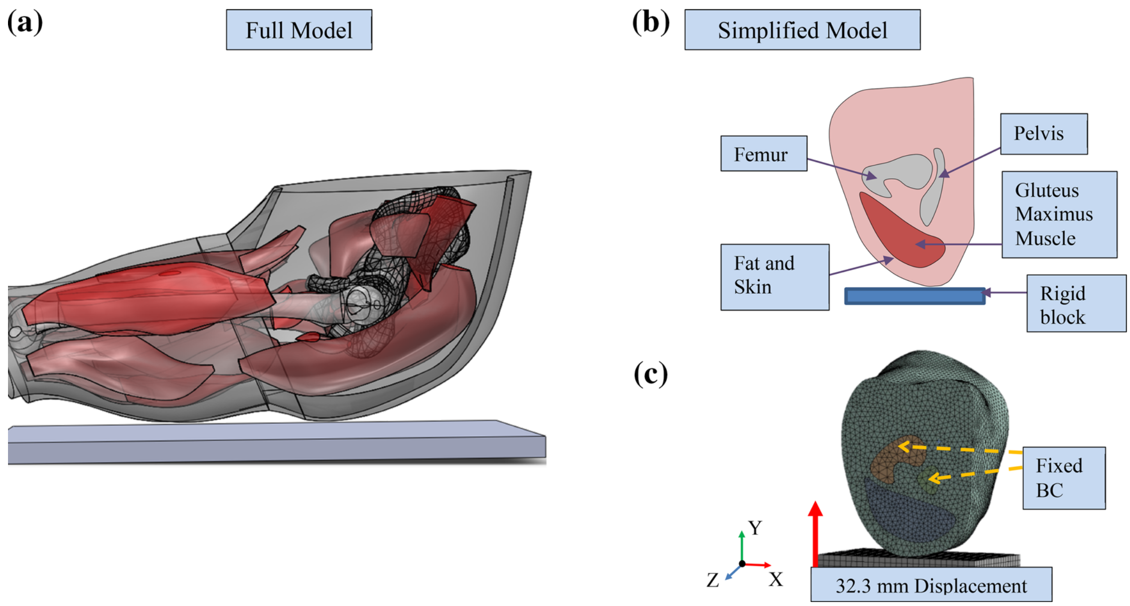

FIGURE 3. An illustration of the detailed (Full) FE model (a) and the simplified FE model (c). (b) The anatomical structures included in the segmentation of the simplified model. (c) The boundary and loading conditions applied to the simplified model.

TABLE 2. Summary of material properties used in the FE model of a seated male.

Soft tissue layer	Formulation	Material properties and model parameters		
Bones	Rigid	$E = 2.5E7$ Pa	$v = 0.3$	Density = 1000 kg m^{-3}
Muscles	Ogden hyper-elastic model	$\mu_1 = 1907.4$ Pa	$\alpha_1 = 4.6$	Density = 1100 kg m^{-3}
Fat and skin	Ogden hyper-elastic model	$\mu_1 = 1166.7$ Pa	$\alpha_1 = 16.2$	Density = 920 kg m^{-3}

Validation of the Developed FE Model

Deformation measured from MRI scans were compared to those estimated by the FE model. To measure the deformation, weight-bearing MRI scans[3] were segmented using ScanIP software (Simpleware Ltd. Exeter, UK) to generate a 3D surface mesh of the deformed muscle. The surface mesh of the deformed muscle was rigidly registered to the undeformed mesh using iterative closest point (ICP) algorithm[30] implemented using Matlab (MathWorks, Inc., Massachusetts, USA). Differences between corresponding nodal coordinated were taken to represent the 3D deformation measured from the MRI scans. Similarly, the FE-deformed mesh (the resultant geometry of the muscle after the FE simulation ran to completion) was registered to the undeformed mesh using ICP and differences in corresponding nodal coordinates were taken to represent the 3D deformation estimated by the FE model. Errors in FE model estimates were calculated as the root mean square of the differences between the MRI-measured and the FE-estimated deformations.

RESULTS

Material Model Parameters Optimisation

Material parameters inferred using GA optimisation are summarised in Table 2. Using Eq. (4), the long-term shear moduli of muscle and fat tissues were estimated to be 1.9 and 1.7 kPa, respectively.

Soft Tissue Deformations

The simulation took 157 min to run. Simulation results showed reasonable estimates of the 3D deformation compared to MRI-based measurement. The mean (±standard deviation) of the root mean square error in the FE estimates of soft tissue deformation was 4.7 mm (±4.4 mm), with about 65% of the deformation estimates being within 5 mm of the MRI-based measurements and less than 13% of the model estimates had errors greater than 10 mm (Fig. 4). The highest errors were noted below the ischial tuberosity.

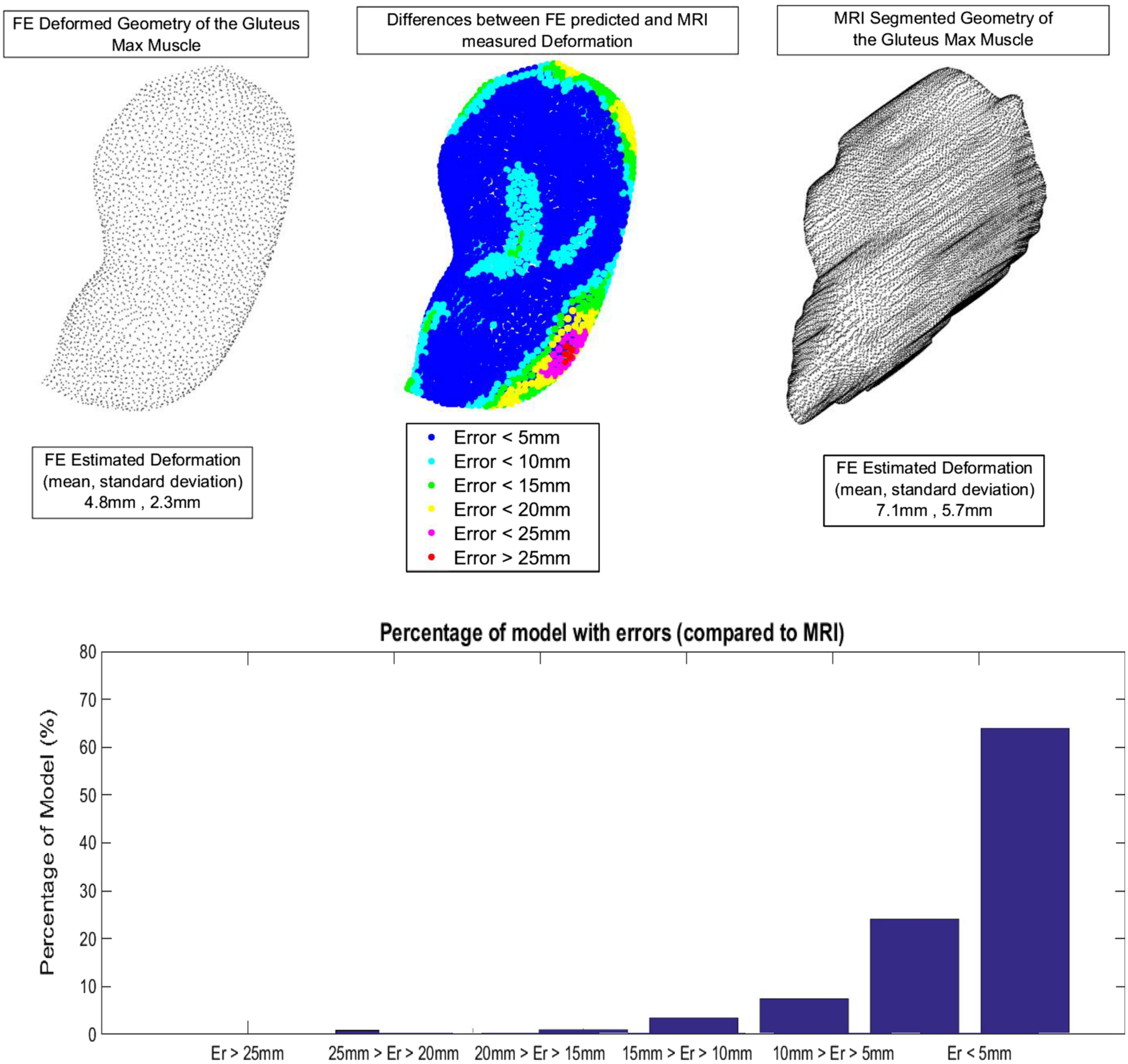

FIGURE 4. FE estimates for soft tissue deformation in the Gluteus Maximus muscle (top-left), MRI measurements of soft tissue deformation in the Gluteus Maximus muscle (top-right) and a contour plot of the distribution of the differences between the FE estimates and the MRI measurements for the deformation in the Gluteus Maximus muscle (top-middle). The legend for contour plot is shown in the bottom-left side of the figure. The bar graph (bottom-right) shows the distribution of the differences (or errors) in the deformation.

Interface Pressure Between the Seat Surface and the Skin

The maximum pressure estimated at the interface between the skin and the rigid seat surface was 31.1 kPa and was located under the ischial tuberosity. The pressure distribution at the interface is shown in Fig. 5.

Compressive Strains

The compressive strains estimated by the FE model were greater for muscles (41%) than for subcutaneous (20%) and inter-muscular fat (21%), with the maxima being in soft tissues close to the ischial tuberosity. Muscles that experienced the highest compressive strains were the gluteus maximus (41%), adductor magnus (21%), biceps femoris (29%), semitendinosus (28%), and semimembranosus (21%) muscles (Fig. 6a).

Shear Strains

The shear strains estimated by the FE model were greater for muscles (110%) than for subcutaneous (58%) and inter-muscular fat (62%). The maximum shear strains the fat components of the model were at

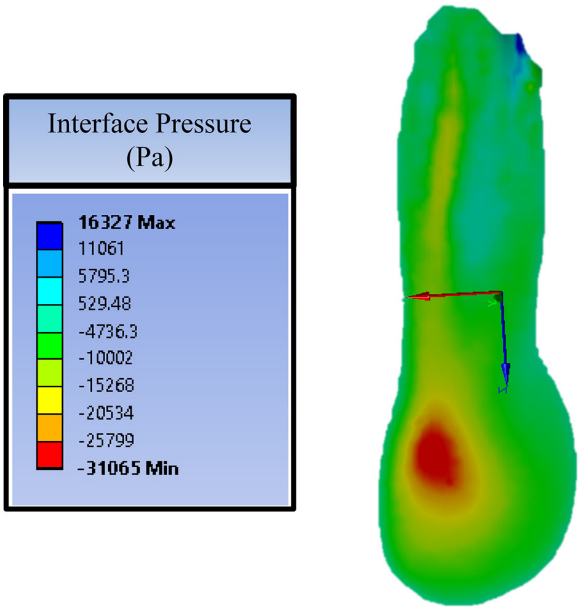

FIGURE 5. FE estimate for the pressure distribution at the seat-buttock interface. The maximum interface pressure was estimated below the ischium with peak value of 31.1 kPa.

the interface between the gluteus maximus muscle and the ischial tuberosity. Muscles that were under the highest strains were the gluteus maximus (110%), adductor magnus (50%), biceps femoris (55%), semitendinosus (50%), and semimembranosus (54%) muscles (Fig. 6b).

von-Mises Strains

The von-Mises strains were greater for muscles than for fat. The highest von-Mises strains in the muscles were in the gluteus maximus (73%), biceps femoris (43%), adductor magnus (29%), semitendinosus (37%), and semimembranosus (37%) (Fig. 6c). The maximum von-Mises strains in the inter-muscular and subcutaneous fat layers did not exceed 41 and 37%, respectively.

DISCUSSION

The aim of this study was to develop and validate an FE model for the buttock and thigh of a seated individual with anatomical detail sufficient for estimating deformation and strains in deep tissues. The developed model was able to estimate the deformation in the gluteal region within (mean ± SD) 4.7 ± 4.4 mm of the MRI-measurements, with more than 65% of the deformation estimates were within 5 mm of the MRI measurements. The strain estimated by the FE model also fell within ranges reported in the literature (Table 3),[11,19–21,24,47] and the FE model produced a physiologically reasonable estimate of loading pattern at the seat interface, with maximum pressure that closely matched interface pressure measurements reported in previous studies.[20,22,57]

Our model appears to produce a better estimation of soft tissue deformation than possible with previous models. The FE model that appears to have the highest geometric detail in the literature was reported in Makhsous *et al.*,[27] which was developed based on MRI scans of a subject in a simulated sitting posture and validated against measurements of the subject's soft tissues deformation (average ± SD errors were 6.2 ± 10.4 mm). Although their model provided valuable information about the distribution of strains in sub-dermal tissues, the resolution was limited to muscle groups/compartments. In contrast, our FE model quantifies the response of individual muscles, inter-muscular and subcutaneous fat and skin to sitting loads, and with higher accuracy when compared to MRI-measurements.

Measurements using the developed FE model suggest that muscles experience higher strains than inter-muscular and subcutaneous fat when exposed to quasi-static sitting loads, indicating that muscles undergo larger deformations than other soft tissues. These results agree with our previous observations[3] and confirm findings reported in previous studies.[22,29,41] The developed FE model has also demonstrated that the highest strains were in the gluteus maximus muscle under the ischial tuberosity and that muscles other than the gluteus maximus were also subjected to relatively high mechanical loads. These muscles were the adductor magnus, biceps femoris, semitendinosus and semimembranosus muscles, which are mainly located in the posterior aspect of the thigh. The relatively high mechanical loads imposed on these muscles can potentially explain the discomfort (or even pain) in the posterior aspect of the thighs after sitting for long hours.[10,32]

Despite the reasonably close estimates of soft tissue deformation, the model seems to underestimate the deformation when compared to the MRI measurements. A localised high underestimation was noted directly below the ischial tuberosity. The MRI measurements indicate that the gluteus maximus muscle entirely slides in the lateral direction, leaving only fat tissues below the ischial tuberosity, however, the FE model did not capture this behaviour. We believe that this could be due to the (simplified) tied/non-slip contact assigned to the muscle-fat interface. Currently, there is paucity in information reported for tissue-on-tissue contact,[38,39] and further research is needed to understand the contact mechanics at the muscle–fat interface.

Long-term shear modulus of elasticity is considered an appropriate parameter to describe the material be-

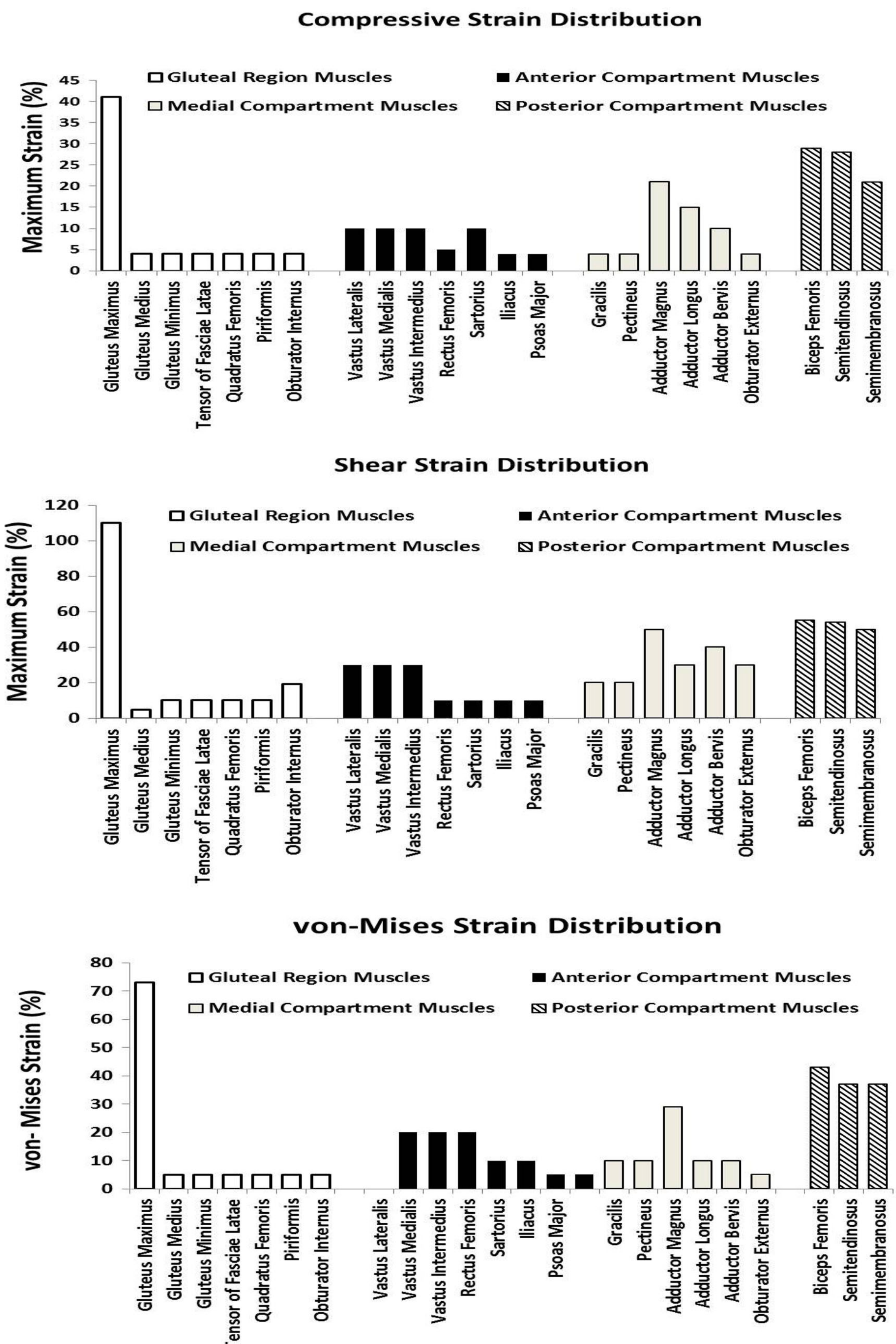

FIGURE 6. Distribution of the compressive (top), shear (middle) and von-Mises (bottom) strains across the different muscles modelled in this FE simulation.

TABLE 3. Summary of the stresses and strains predicted by the FE model and the literature cited range for each of the predicted stresses and strains.

	Inter-muscular fat		Muscles		Fat and skin	
	FE model	Literature	FE model	Literature	FE Model	Literature
Maximum compressive strains (%)	21	–	41	7–90	20	15–83
Maximum von-Mises strains (%)	41	–	79	59–140	37	19–52
Maximum shear strains (%)	62	–	110	51–118	58	17–63

Literature: [17,40–44,46].

haviour under quasi-static loading.[48] In this study, the long-term shear moduli for muscle and fat tissues were estimated from optimised material parameter values. Based on the estimated values of shear moduli, muscles and fat seem to exhibit similar response to quasi-static loading. However, the optimal material parameters in this study do not only represent material properties of muscle and fat tissues, they also compensate for the simplified contact definition and loading conditions applied to the FE model. Therefore, the reported values for shear moduli should not be taken as exact measurements of subject-specific material properties. Nonetheless, the shear moduli estimated in this study were consistent with values reported in studies that measured shear moduli of muscles and fat tissues, *in vivo* on human subjects.[4,44,50,51,53] This implies that despite the inherent limitations, the proposed method seems to be provide reasonable estimates for shear moduli of muscle and fat tissues. Future work is needed to differentiate (if possible) between material properties and the boundary conditions described by the optimised material models.

There were several limitations in this study. The models assumed a symmetric behaviour of soft tissues for seated individuals. Soft tissues were also assumed to be homogeneous isotropic materials, which does not consider the possible heterogeneity across the different regions of the model, nor accounts for anisotropy due to muscle fibre direction. Also, the loading and boundary conditions applied to the model were highly simplified. Ideally, interface pressure would be measured while the subject is scanned then used as the loading condition for the model instead of the simplified purely vertical displacement of the seat surface. However, this was not possible because commercially available pressure mats are not MRI-compatible. Also, the contact definition assigned to the muscle-to-fat and fat-to-bone interfaces were simplified. A tied/non-slip contact was assumed at the muscle-to-fat interface and the fat-to-bone interface. These boundary conditions affect the distribution of shear and compressive load components across the various soft tissue layers between the bones and the seat surface. However, investigation of how variations in the assumed boundary conditions affect the FE estimates is outside the scope of this study.

The developed FE model was validated against MRI measurements of soft tissue deformation, however, only for the gluteal region of the model. This was because MRI data in the weight-bearing posture only captured the gluteal region of the buttock and thighs. While this assesses the validity of the model's predictions in the gluteal region, it does not guaranty the validity of the model in predicting the deformation in other regions, such as the distal thighs. Future research may consider expanding the validation presented to evaluate the accuracy of the model in predicting the deformation in other regions of the buttock and thigh.

The developed model can inform seat and cushion designers about how sub-dermal tissues would behave in new seat and cushion designs. Different variations may be investigated, and depending on the needs of the targeted users, designers would be able to make informed decisions on how to improve seat and cushion design. However, stress/strain criteria for injury or discomfort are not clearly defined in the literature.[36] Once such criteria become available, the developed model can provide insight that would help designers improve seat design to meet the needs of different users.[15]

CONCLUSION

We have presented the development and validation of a unique three-dimensional, subject-specific FE model with high anatomical fidelity for a seated human. The current FE model provides insight into the distribution of sub-dermal strains in individual muscles, inter-muscular and subcutaneous fat layers. When compared to deformations measured using MRI, the accuracy of the developed model was higher than what is reported for previous three-dimensional FE models in the literature. FE estimate of the mechanical strains in muscles and fat tissues suggest that, for a seated human, the gluteus maximus, adductor magnus and posterior compartment muscles bear the highest mechanical loads.

ACKNOWLEDGMENT

AutoCRC and the Maurice de Rohan Scholarship funded this research.

REFERENCES

[1]Akimoto, M., T. Oka, K. Oki, and H. Hyakusoku. Finite element analysis of effect of softness of cushion pads on stress concentration due to an oblique load on pressure sores. *J. Nippon Med. Sch.* 74:230–235, 2007.

[2]Al-Dirini R., M. Reed, G. Paul, and D. Thewlis. A subject-specific model of human buttocks and thighs in a seated posture. *ACAM 7*. Adelaide, 2012.

[3]Al-Dirini, R. M., M. P. Reed, and D. Thewlis. Deformation of the gluteal soft tissues during sitting. *Clin. Biomech.* 30:662–668, 2015.

[4]Bensamoun, S. F., S. I. Ringleb, L. Littrell, Q. Chen, M. Brennan, R. L. Ehman, and K. N. An. Determination of thigh muscle stiffness using magnetic resonance elastography. *J. Magn. Reson Imaging* 23:242–247, 2006.

[5]Bidar, M., R. Ragan, T. Kernozek, and J. Matheson. Finite element calculation of seat-interface pressures for various wheelchair cushion thicknesses. *Univ. Wis. La Crosse J. Undergrad. Res.* 3:277–280, 2000.

[6]British Chiropractic Association. Nation is Bending Over Backwards at Work. 2006.

[7]Brosh, T., and M. Arcan. Modeling the body/chair interaction—an integrative experimental–numerical approach. *Clin. Biomech.* 15:217–219, 2000.

[8]Ceelen, K., A. Stekelenburg, S. Loerakker, G. Strijkers, D. Bader, K. Nicolay, F. Baaijens, and C. Oomens. Compression-induced damage and internal tissue strains are related. *J. Biomech.* 41:3399–3404, 2008.

[9]Choi, H. Y., K. M. Kim, J. Han, S. Sah, S. H. Kim, S. H. Hwang, K. N. Lee, J. K. Pyun, N. Montmayeur, and C. Marca. Human body modeling for riding comfort simulation. Berlin: Springer, pp. 813–823, 2007.

[10]Dhingra, H., V. Tewari, and S. Singh. Discomfort, pressure distribution and safety in operator's seat—a critical review. *Agric. Eng. Int.* 5:1–16, 2003.

[11]Elsner, J. J., and A. Gefen. Is obesity a risk factor for deep tissue injury in patients with spinal cord injury? *J. Biomech.* 41:3322–3331, 2008.

[12]Fletcher A. and P. Mitchell. Fatigue-related risks for Queensland taxi drivers—final report on the operational and scientific factors related to fatigue in taxi drivers, to inform the possible development of reform, regulation and industry guidelines, edited by Q. Government Integrated Safety Support, 2011, pp. 1–22.

[13]Grieco, A. Sitting posture: an old problem and a new one. *Ergonomics* 29:345–362, 1986.

[14]Hu, J., K. D. Klinich, C. S. Miller, J. D. Rupp, G. Nazmi, M. D. Pearlman, and L. W. Schneider. A stochastic visco-hyperelastic model of human placenta tissue for finite element crash simulations. *Ann. Biomed. Eng.* 39:1074–1083, 2011.

[15]Hu, J., J. D. Rupp, and M. P. Reed. Focusing on vulnerable populations in crashes: recent advances in finite element human models for injury biomechanics research. *J. Automot. Saf. Energy* 3:295–307, 2012.

[16]Iwamoto, M., Y. Nakahira, H. Kimpara, T. Sugiyama, and K. Min. Development of a human body finite element model with multiple muscles and their controller for estimating occupant motions and impact responses in frontal crash situations. *Stapp Car Crash J.* 56:231, 2012.

[17]Kohandel, M., S. Sivaloganathan, and G. Tenti. Estimation of the quasi-linear viscoelastic parameters using a genetic algorithm. *Math. Comput. Model.* 47:266–270, 2008.

[18]Laurent, V., C. Then, and G. Silber. Human modeling and CAE based subjective seat comfort score correlation. *Int. J. Commer. Veh.* 7:295–304, 2014.

[19]Lim D., F. Lin, R. Hendrix, and M. Makhsous. Finite element analysis for evaluation of internal mechanical responses in buttock structure in a true sitting posture: development and validation. *RESNA 29th International conference*, 2006, pp. 22–26.

[20]Lim, D., F. Lin, R. W. Hendrix, B. Moran, C. Fasnati, and M. Makhsous. Evaluation of a new sitting concept designed for prevention of pressure ulcer on the buttock using finite element analysis. *Med. Biol. Eng. Comput.* 45:1079–1084, 2007.

[21]Linder-Ganz, E., and A. Gefen. Mechanical compression-induced pressure sores in rat hindlimb: muscle stiffness, histology, and computational models. *J. Appl. Physiol.* 96:2034–2049, 2004.

[22]Linder-Ganz, E., N. Shabshin, Y. Itzchak, and A. Gefen. Assessment of mechanical conditions in sub-dermal tissues during sitting: a combined experimental-MRI and finite element approach. *J. Biomech.* 40:1443–1454, 2007.

[23]Linder-Ganz, E., N. Shabshin, Y. Itzchak, Z. Yizhar, I. Siev-Ner, and A. Gefen. Strains and stresses in sub-dermal tissues of the buttocks are greater in paraplegics than in healthy during sitting. *J. Biomech.* 41:567–580, 2008.

[24]Linder-Ganz, E., G. Yarnitzky, Z. Yizhar, I. Siev-Ner, and A. Gefen. Real-time finite element monitoring of sub-dermal tissue stresses in individuals with spinal cord injury: toward prevention of pressure ulcers. *Ann. Biomed. Eng.* 37:387–400, 2009.

[25]Loerakker, S., D. L. Bader, F. Baaijens, and C. Oomens. Which factors influence the ability of a computational model to predict the in vivo deformation behaviour of skeletal muscle? *Comput. Method. Biomech. Biomed. Eng.* 16:338–345, 2013.

[26]Luboz, V., M. Petrizelli, M. Bucki, B. Diot, N. Vuillerme, and Y. Payan. Biomechanical modeling to prevent ischial pressure ulcers. *J. Biomech.* 47:2231–2236, 2014.

[27]Makhsous, M., D. Lim, R. Hendrix, J. Bankard, W. Z. Rymer, and F. Lin. Finite element analysis for evaluation of pressure ulcer on the buttock: development and validation. *IEEE Trans. Neural Syst. Rehabil. Eng.* 15:517–525, 2007.

[28]Makhsous, M., and F. Lin. Bioengineering research of chronic wounds. In: A Finite-Element Biomechanical Model for Evaluating Buttock Tissue Loads in Seated Individuals with Spinal Cord Injury, edited by A. Gefen. Berlin: Springer, 2009, pp. 181–205.

[29]Makhsous, M., F. Lin, A. Cichowski, I. Cheng, C. Fasanati, T. Grant, and R. W. Hendrix. Use of MRI images to measure tissue thickness over the ischial tuberosity at different hip flexion. *Clin. Anat.* 24:638–645, 2011.

[30]Manu and E. Audenaert. Rigid ICP registration. *Matlab Cetral File Exchange Mathworks*, 2015.

[31]Mayhew C. and M. Quinlan. Occupational health and safety amongst 300 long distance truck drivers: results of an

interview-based survey. *Report of Inquiry into Safety in the Long Haul Trucking Industry,* 2000.
[32]Mehta, C., and V. Tewari. Seating discomfort for tractor operators—a critical review. *Int. J. Ind. Ergon*. 25:661–674, 2000.
[33]Mergl, C., T. Anton, R. Madrid-Dusik, J. Hartung, A. Liberandi, and H. Bubb. Development of a 3D finite element model of thigh and pelvis. In: SAE Digital Human Modeling for Desing and Engineering Symposium, edited by SAE. Rochester: Oakland University, 2004.
[34]Mills, N. Polymer Foams Handbook: Engineering and Biomechanics Applications and Design Guide. Boston: Butterworth-Heinemann, 2007.
[35]Ogden, R. W. Non-linear Elastic Deformations. New York: Courier Dover Publications, 1997.
[36]Olesen, C. G., M. de Zee, and J. Rasmussen. Missing links in pressure ulcer research—an interdisciplinary overview. *J. Appl. Physiol*. 108:1458–1464, 2010.
[37]Petru, M. P. Development and optimization of the headrests seat according the signal Whiplash. *Bull. Appl. Mech.* 6:34–40, 2010.
[38]Portnoy, S., I. Siev-Ner, N. Shabshin, A. Kristal, Z. Yizhar, and A. Gefen. Patient-specific analyses of deep tissue loads post transtibial amputation in residual limbs of multiple prosthetic users. *J. Biomech*. 42:2686–2693, 2009.
[39]Portnoy, S., J. van Haare, R. P. Geers, A. Kristal, I. Siev-Ner, H. A. Seelen, C. W. Oomens, and A. Gefen. Real-time subject-specific analyses of dynamic internal tissue loads in the residual limb of transtibial amputees. *Med. Eng. Phys.* 32:312–323, 2010.
[40]Ragan, R., T. W. Kernozek, M. Bidar, and J. Matheson. Seat-interface pressures on various thicknesses of foam wheelchair cushions: a finite modeling approach. *Arch. Phys. Med. Rehabil*. 83:872–875, 2002.
[41]Shabshin, N., G. Zoizner, A. Herman, V. Ougortsin, and A. Gefen. Use of weight-bearing MRI for evaluating wheelchair cushions based on internal soft-tissue deformations under ischial tuberosities. *J. Rehabil. Res. Dev*. 47:31–42, 2010.
[42]Shacham, S., D. Castel, and A. Gefen. Measurements of the static friction coefficient between bone and muscle tissues. *J. Biomech. Eng*. 132:084502, 2010.
[43]Siefert A., S. Pankoke, and H. P. Wölfel. Detailed 3D muscle approach for computing dynamic loads on the lumbar spine for implant design. *IFMBE*, 2010.
[44]Silber, G., and C. Then. Human body models: Boss-models. Berlin: Springer, pp. 175–244, 2013.
[45]Silber, G., and C. Then. Preventive Biomechanics. Berlin: Springer, 2013.
[46]Sonenblum, S. E., S. H. Sprigle, J. M. Cathcart, and R. J. Winder. 3-Dimensional buttocks response to sitting: a case report. *J. Tissue Viability* 22:12–18, 2013.
[47]Sopher, R., J. Nixon, C. Gorecki, and A. Gefen. Exposure to internal muscle tissue loads under the ischial tuberosities during sitting is elevated at abnormally high or low body mass indices. *J. Biomech*. 43:280–286, 2010.
[48]Sopher, R., J. Nixon, C. Gorecki, and A. Gefen. Effects of intramuscular fat infiltration, scarring, and spasticity on the risk for sitting-acquired deep tissue injury in spinal cord injury patients. *J. Biomech. Eng*. 133:021011, 2011.
[49]Stockton, L., and D. Parker. Pressure relief behaviour and the prevention of pressure ulcers in wheelchair users in the community. *J. Tissue Viability* 12(84):88–90, 2002.
[50]Then, C., J. Menger, G. Benderoth, M. Alizadeh, T. Vogl, F. Hübner, and G. Silber. A method for a mechanical characterisation of human gluteal tissue. *Technol. Health Care* 15:385–398, 2007.
[51]Todd, B. A., and J. G. Thacker. Three-dimensional computer model of the human buttocks, in vivo. *J. Rehabil. Res. Dev*. 31:111, 1994.
[52]Tremblay, M. S., R. C. Colley, T. J. Saunders, G. N. Healy, and N. Owen. Physiological and health implications of a sedentary lifestyle. *Appl. Physiol. Nutr. Metab*. 35:725–740, 2010.
[53]Untaroiu C., K. Darvish, J. Crandall, B. Deng, and J. T. Wang. Characterization of the lower limb soft tissues in pedestrian finite element models. *19th International Technical Conference on the Enhanced Safety of Vehicles,* 2005.
[54]Untaroiu, C. D., and Y.-C. Lu. Material characterization of liver parenchyma using specimen-specific finite element models. *J. Mech. Behav. Biomed. Mater*. 26:11–22, 2013.
[55]Untaroiu C. D., Y.-C. Lu, and A. R. Kemper. Modeling the biomechanical and injury response of human liver parenchyma under tensile loading. *Proceeding of the IRCOBI Conference, Goteborg, Sweden*, 2013.
[56]Untaroiu, C. D., N. Yue, and J. Shin. A finite element model of the lower limb for simulating automotive impacts. *Ann. Biomed. Eng*. 41:513–526, 2013.
[57]Verver, M., J. Van Hoof, C. Oomens, J. Wismans, and F. Baaijens. A finite element model of the human buttocks for prediction of seat pressure distributions. *Comput. Methods Biomech. Biomed. Eng*. 7:193–203, 2004.
[58]Wall, J. Preventing pressure sores among wheelchair users. *Prof. Nurse* 15:321–324, 2000.
[59]Zhang, M., and A. Mak. In vivo friction properties of human skin. *Prosthet. Orthot. Int*. 23:135–141, 1999.